Received: 30 April 2021 | Revised: 9 July 2021 | Accepted: 12 July 2021

DOI: 10.1111/cas.15074

ORIGINAL ARTICLE

Cancer Science WILEY

Inhibition of MEK pathway enhances the antitumor efficacy of chimeric antigen receptor T cells against neuroblastoma

Akimasa Tomida[1] | Shigeki Yagyu[1,2] | Kayoko Nakamura[3] | Hiroshi Kubo[1] | Kumiko Yamashima[4] | Yozo Nakazawa[2,3,5] | Hajime Hosoi[1] | Tomoko Iehara[1]

[1]Department of Pediatrics, Kyoto Prefectural University of Medicine, Graduate School of Medical Science, Kyoto, Japan

[2]Center for Advanced Research of Gene and Cell Therapy in Shinshu University (CARS), Shinshu University School of Medicine, Matsumoto, Japan

[3]Department of Pediatrics, Shinshu University School of Medicine, Matsumoto, Japan

[4]Division of Cancer Immunotherapy, Exploratory Oncology Research and Clinical Trial Center, National Cancer Center, Kashiwa, Japan

[5]Institute for Biomedical Sciences, Interdisciplinary Cluster for Cutting Edge Research, Shinshu University, Matsumoto, Japan

Correspondence
Shigeki Yagyu, Department of Pediatrics, Kyoto Prefectural University of Medicine, Graduate School of Medical Science, Kyoto, Japan
Email: shigeky@koto.kpu-m.ac.jp

Funding information
Japan Society for the Promotion of Science, Grant/Award Number: 20K07461

Abstract

Disialoganglioside (GD2)-specific chimeric antigen receptor (CAR)-T cells (GD2-CAR-T cells) have been developed and tested in early clinical trials in patients with relapsed/refractory neuroblastoma. However, the effectiveness of immunotherapy using these cells is limited, and requires improvement. Combined therapy with CAR-T cells and molecular targeted drugs could be a promising strategy to enhance the antitumor efficacy of CAR T cell immunotherapy. Here, we generated GD2-CAR-T cells through *piggyBac* transposon (PB)-based gene transfer (PB-GD2-CAR-T cells), and analyzed the combined effect of these cells and a MEK inhibitor in vitro and in vivo on neuroblastoma. Trametinib, a MEK inhibitor, ameliorated the killing efficacy of PB-GD2-CAR-T cells in vitro, whereas a combined treatment of the two showed superior antitumor efficacy in a murine xenograft model compared to that of PB-GD2-CAR-T cell monotherapy, regardless of the mutation status of the MAPK pathway in tumor cells. The results presented here provide new insights into the feasibility of combined treatment with CAR-T cells and MEK inhibitors in patients with neuroblastoma.

KEYWORDS

CAR-T cell therapy, chimeric antigen receptor, GD2, MEK inhibitor, neuroblastoma, trametinib

1 | INTRODUCTION

Chimeric antigen receptor-T (CAR-T) cell therapy redirected to a specific antigen on tumor cells is a promising treatment strategy for relapsed/refractory tumors, which cannot be cured by current standard treatments. Chimeric antigen receptor-T cell therapy specific to CD19 has achieved considerable success in a subset of patients with highly refractory B cell tumors,[1-4] and various CAR-T cell products are being used for other cancers including solid tumors.[5,6] Disialoganglioside GD2 is strongly expressed on tumors of neuroectodermal origin, including human neuroblastoma (NB) and melanoma, but its expression on normal tissues is very weak.[7-9] Therefore, GD2 is a suitable target of CAR-T cell therapy of NB. GD2-specific CAR-T (GD2-CAR-T) cells have been developed and tested in early clinical trials[10-13]; however, their effectiveness is limited partly because of exhaustion,[14] actively hostile tumor microenvironment,[15,16] and immune evasion due to the expression of immunosuppressive molecules, such as programmed cell death 1 ligand (PD-L1), on the surface of tumor cells.[17-20]

Therefore, further modification of GD2-CAR-T cells or combined therapies with immune checkpoint inhibitors are attractive therapeutic options and have been evaluated in preclinical models and clinical trials to increase the efficacy of CAR-T cells.[13,21,22]

Because relapsed/refractory NB cells accumulate genetic mutations related to the cellular proliferation machinery, molecular-targeting therapy to obstruct the essential pathway of malignant transformation could be an attractive therapeutic method. One promising strategy would be to block the MAPK pathway, considering that relapsed high-risk NBs show frequent mutations in the RAS-MAPK pathway.[23] Mitogen-activated protein kinase kinase inhibitors have shown promising antitumor efficacy for high-risk NB in preclinical models and clinical trials.[24-27]

The MEK inhibitors achieved high but short-lived response rates for patients with MAPK pathway mutated melanoma.[28] By contrast, immunotherapies, including those with immune checkpoint inhibitors (ICIs), showed lower response rates but more durable responses.[29,30] Recently, it has been shown that combination of MEK inhibitors with PD-1 blockade improves the antitumor activity in preclinical models and achieves sustained remission in patients with melanoma[31,32]; such combinations could provide additional treatment options for patients unlikely to have long-lasting responses to either mode of therapy alone. Because the immune evasion mechanism in tumor cells or in the tumor microenvironment is partially regulated by the MAPK pathways in several cancer cells,[31,33-35] we hypothesized that inhibition of MAPK signaling pathways would enhance the efficacy of CAR-T cell therapy. We developed GD2-CAR-T cells by *piggyBac* transposon (PB)-based gene transfer and evaluated whether combination therapy of these cells with MEK inhibitors would improve their killing activity against NB.

2 | MATERIALS AND METHODS

2.1 | Ethics approval and consent to participate

This study was approved by the Institutional Review Board of Kyoto Prefectural University of Medicine (approval numbers: 2019-111 and 2019-112). All experiments involving human participants were carried out in accordance with the Declaration of Helsinki guidelines. Blood samples from healthy donors were obtained with written informed consent using the protocol approved by the Institutional Review Board of Kyoto Prefectural University of Medicine (approval numbers: ERB-C-669 and ERB-C-1406). All animal experiments and procedures were approved by the Kyoto Prefectural University of Medicine Institutional Review Board (permit no. M30-140).

2.2 | Tumor cell lines and blood samples

Three human NB cell lines, SK-N-AS (CRL-2137), SH-SY5Y (CRL-2266), and IMR32 (CRL-127), were purchased from ATCC. The cells were maintained in DMEM (Nacalai Tesque) supplemented with 10% FBS (Invitrogen) and 1% penicillin-streptomycin (Cytiva) at 37°C in an atmosphere of 5% CO_2. The mutation status of the RAS/MEK pathway was determined using the Catalogue of Somatic Mutations in Cancer database (http://cancer.sanger.ac.uk/cell_lines) or previous reports,[24,25,36] and is summarized in Table S1. To obtain a single cell-derived GD2-high SK-N-AS cell clone, parent SK-N-AS cells were stained with phycoerythrin (PE)-conjugated anti-human GD2 Ab (BioLegend), and GD2-high SK-N-AS cells (AS-High) were purified by flow cytometry using a Sony SH800S cell sorter (Sony Biotechnologies). The AS-High cells were further purified through limiting dilution by seeding these cells into 96-well plates at a density of 0.5 cells/100 μL. After formation, single cell-derived colonies were passaged and expanded for further experiments. AS-High and SH-SY5Y cells expressing firefly luciferase (FFluc) (AS-High-FFluc and SY5Y-FFLuc, respectively) were obtained by introducing PB-based pIRII-FFLuc-puroR-GFP, which encodes the FFLuc gene, puromycin resistance gene, and GFP gene, on these cells by electroporation, and subsequent cloning to obtain a single cell-derived clone.

Blood samples were obtained from healthy donors, and PBMCs were immediately isolated by density gradient centrifugation using Lymphocyte Separation Medium 1077 (FUJIFILM Wako Pure Chemical Corporation), followed by multiple washes in PBS (Nacalai Tesque) for the generation of CAR-T cells. The number of live cells was determined using standard Trypan blue staining and Automated Cell Counter model R1 (Olympus).

2.3 | Pharmacologic agents

The MEK1/2 inhibitor, trametinib (GSK12021101), and a dual Raf/MEK inhibitor, CH5126766 (RO5126766), were purchased from ChemScene and Selleckchem, respectively. Both these drugs were solubilized in DMSO to prepare stock solutions, per the manufacturer's protocol.

2.4 | Plasmid construction

The previously described pCMV-PB plasmid encoding PB transposase[37] was artificially synthesized (Mediridge). The pIRII-GD2.CAR plasmid, encoding the GD2-specific single chain fragment variable (scFv, 14G2a), followed by the short hinge CH2CH3 domain of human IgG1, the signaling domain of the CD28 costimulatory molecule, and the ζ-signaling domain of the T-cell receptor complex (TCR), was kindly provided by Dr Cliona M. Rooney (Baylor College of Medicine) and was subcloned into the pIRII transposon vector backbone (pIRII-GD2-28z) (Figure 1A).[11,12] For in vivo experiments, the GD2-28z construct, lacking the IgG1-CH2CH3 spacer region, was synthesized and subcloned into the pIRII transposon vector.

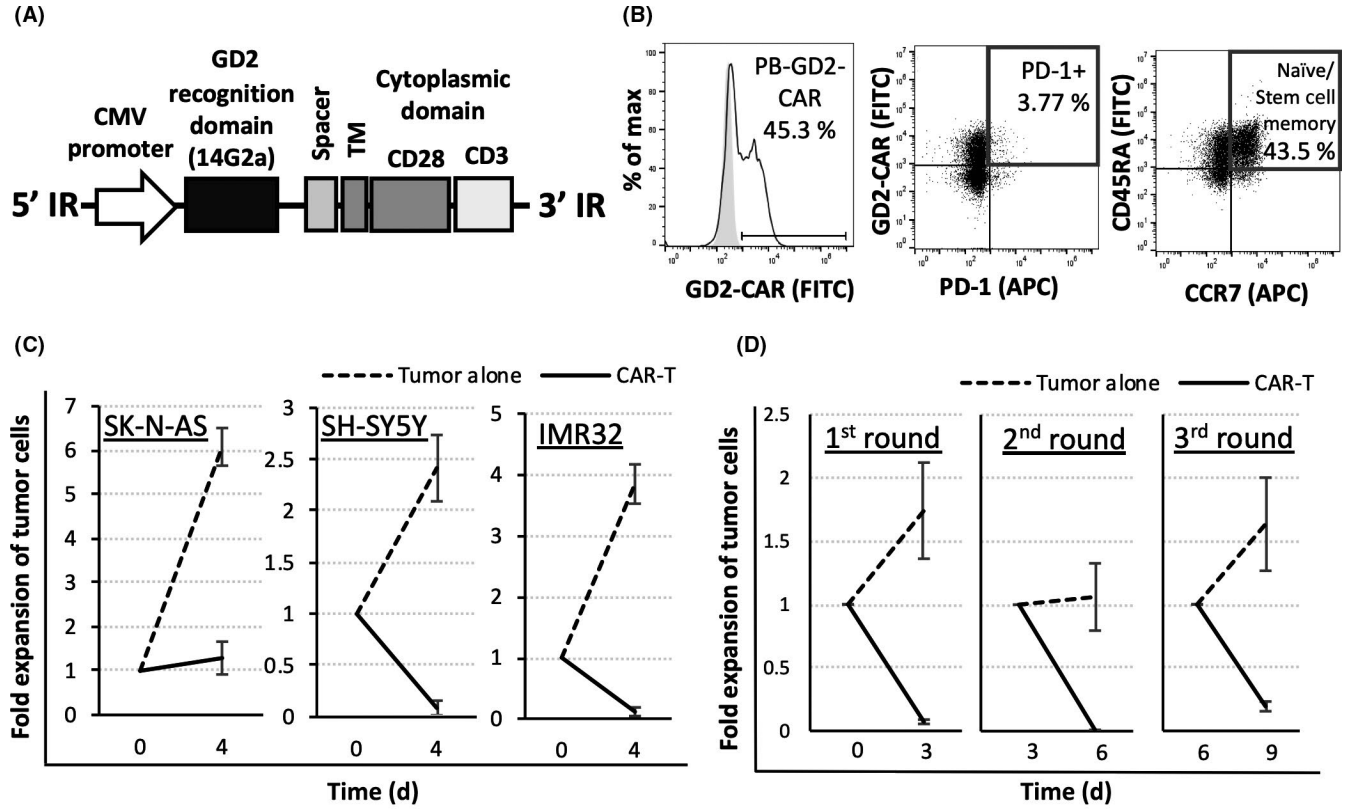

FIGURE 1 Generation of *piggyBac*-mediated disialoganglioside GD2-specific chimeric antigen receptor-T (PB-GD2-CAR-T) cells and their characteristics. A, Schematics of transposon vector expressing the GD2-CAR construct. IR, inverted repeat; TM, trans membranous domain. B, Representative flow cytometry dot plots of the characteristics of PB-GD2-CAR-T cells regarding CAR expression, programmed cell death-1 (PD-1) expression, and differentiation profiles in CAR-T cells on day 14. APC, allophycocyanin. C, Coculture assay. Neuroblastoma and PB-GD2-CAR-T cells were cocultured for 4 days at an effector : target (E:T) ratio of 2:1. The number of live tumor cells ($GD2^+$, $CD3^-$ cell fraction) were measured by flow cytometry using counting beads (mean ± SD, n = 3). D, Sequential coculture assay. In the first round, SH-SY5Y and PB-GD2-CAR-T cells were cocultured for 3 days at an E:T ratio of 2:1. For the second and third cocultures, the same number of fresh SH-SY5Y and PB-GD2-CAR-T cells as used in the previous round, were used at the same E:T ratio

2.5 | Generation of PB-mediated GD2-CAR-T cells

The CAR transgene was transduced into fresh, unstimulated PBMCs using the PB transposon system, as described previously.[38] Briefly, 2 × 107 fresh, unmanipulated PBMCs were electroporated with pCMV-PB (7.5 μg) and pIRII-GD2-28z (7.5 μg) using 4D-Nucleofector and the P3 Primary Cell 4D-Nucleofector X kit (program FI-115; Lonza) on day 0, and cultured in complete culture medium (CCM) consisting of ALyS 705 Medium (Cell Science & Technology Institute) supplemented with 5% artificial serum (Animal-free; Cell Science & Technology Institute), interleukin-7 (IL-7, 10 ng/mL; Miltenyi Biotec), and IL-15 (5 ng/mL, Miltenyi Biotec) at 37°C in a humidified incubator with 5% CO_2 atmosphere for 24 hours. Simultaneously, 5 × 106 fresh, unmanipulated PBMCs from the same donor were pulsed with 24-well plate coated with 0.05 μg/mL of MACS PepTivator AdV5 Hexon, CMVpp65, EBNA-1, and BZLF1, for 30 minutes. Thereafter, these cells were UV-irradiated for inactivation, and cocultured with CAR-T cells in CCM. On day 7, these cells were transferred to an anti-CD3 or anti-CD28 mAb-coated plate, and cultured in CCM for 48 hours. On day 9, these cells were transferred and expanded in G-Rex 6 Multi-Well Cell Culture Plates (Wilson Wolf Corporation) until day 14.

2.6 | Flow cytometry

The expression of GD2 on the tumor cell lines was determined by staining with PE-conjugated human anti-GD2 Ab (BioLegend). Allophycocyanin (APC)-conjugated human anti-PD-L1 and anti-human leukocyte antigen (HLA) A, B, C Abs (all from BioLegend) were used for the evaluation of PD-L1 and HLA class I on the tumor cells, respectively. Cell surface expression of GD2-CAR on PB-GD2-CAR-T cells, which has the IgG CH2CH3 spacer region, was determined using an FITC-conjugated goat anti-human IgG Fc fragment-specific Ab (Merck Millipore), or FITC-conjugated goat $F(ab')_2$ anti-mouse $IgG(Fab')_2$ Ab (Abcam) for the CAR-T cells lacking the IgG CH2CH3 spacer region. The FITC-conjugated Ab against CD45RA, APC-conjugated Abs against CD3, CCR7, PD-1, and Tim3, and Alexa Fluor 647 anti-LAG3 Ab (all from BioLegend) were used for characterizing the phenotype of CAR-T cells. Detailed information of recombinant proteins and Abs used is provided in Table S2.

All flow cytometry data were acquired using BD FACS Accuri C6 Plus (BD Biosciences) and analyzed using FlowJo Software (Tree Star).

2.7 | Cytotoxicity assay

An in vitro killing assay was carried out using xCELLigence Real Time Cell Analysis Technology (ACEA Biosciences). Briefly, after measurement of the background impedance, 1.5×10^4 NB cells were seeded onto an E-plate 16 (ACEA Biosciences). Approximately 24 hours after seeding, 3×10^4 GD2-CAR-T cells were added in combination with trametinib. The real-time impedance was measured for 96 hours and presented as the normalized cell index using the xCELLigence RTCA DP system and the data were analyzed using xCELLigence RTCA Software version 2.0 (ACEA Biosciences).

2.8 | Sequential killing assay

Sequential killing assays were carried out by adding fresh tumor cells into CAR-T cells cocultured with tumor cells every 3 days by restoring an effector : target (E:T) ratio of 2:1. Thereafter, the cell mixture was collected, stained with PE-conjugated anti-human GD2 Ab and APC-conjugated anti-CD3 Ab to identify the NB and T cells, respectively, and mixed with 50 000 CountBright Absolute Counting Beads (Thermo Fisher Scientific). The number of live tumor cells ($GD2^+$, $CD3^-$ cell fraction) was measured by flow cytometry until the number of counting beads reached 5000.

2.9 | Cytokine release assay

To explore the response of CAR-T cells against the target cells, the production of γ-interferon (IFN-γ) and tumor necrosis factor (TNF) was measured using a Cytometric Bead Array Kit (BD Biosciences). Briefly, tumor cells were cocultured with CAR-T cells at an E:T ratio of 2:1. After 48 hours of coculture, the cell culture supernatant was collected, and the concentration of cytokines was measured and analyzed. Data were acquired on BD Accuri C6 Plus and analyzed using the FCAP Array version 3.0 software.

2.10 | Intracellular staining

The phosphorylation of ERK1/2 of CAR-T cells was measured by intracellular staining. The CAR-T cells were stimulated with anti-CD3/CD28 mAb-coated plates for 48 hours, in the presence of trametinib or DMSO, respectively. The cells were then fixed in BD Cytofix Fixation Buffer (BD Biosciences), washed and permeabilized with BD Phosflow Perm Buffer II (BD Biosciences) according to the manufacturer's protocol, and washed twice with staining buffer. For flow cytometry analysis, cells were stained with APC-conjugated mouse anti-human CD3 and PE-conjugated mouse anti-ERK1/2 (pY202/pY204) Ab for 30 minutes in the dark at room temperature. Data were acquired on BD Accuri C6 Plus and analyzed using FlowJo software.

2.11 | In vivo xenograft NB model

Female, 4-week-old, CB17.Cg-*Prkdc*^{scid}*Lyst* $^{bg\text{-}J}$/CrlCrlj (SCID Beige) mice were purchased from Japan Oriental BioService and housed at the Kyoto Prefectural University of Medicine for over 1 week before the experiment. Food and water were available ad libitum. AS-High-FFLuc and SY5Y-FFLuc cells were suspended in a total volume 100 μL Matrigel Matrix (Corning) to prepare 5×10^6 cells, and subcutaneously injected into the dorsal wall of the mice. After tumor inoculation, the mice were randomized into a nontherapy group (vehicle alone), a trametinib monotherapy group, a GD2-CAR-T cell group, and a trametinib with CAR-T cell group. Approximately 2×10^6 GD2-CAR-T cells were intravenously injected into mice through the tail vein. Tumor growth was measured as bioluminescence signal intensity following intraperitoneal injection with D-luciferin (Cayman Chemical) and expressed as total flux (p/s) using the IVIS imaging system (PerkinElmer). Image analysis and quantification of bioluminescence were carried out using Living Image software (PerkinElmer). Mice were killed when predefined end-points or euthanasia criteria were met in accordance with the Center for Comparative Medicine at the Kyoto Prefectural University of Medicine.

2.12 | Statistical analysis

Data are represented as mean ± SD. Statistical significance was defined as $P < .05$. Two-tailed Student's *t* test was used to determine the statistical significance of differences between samples. Log-rank test was used to compare survival curves obtained using the Kaplan-Meier method. Statistical analyses were undertaken using the GraphPad Prism 7 software.

3 | RESULTS

3.1 | Generation and characterization of GD2-specific CAR-T cells by PB transposon-based gene transfer

Unstimulated PBMCs were transfected with the GD2-CAR transgene (Figure 1A) and the PB transposase gene using electroporation, and cultured according to the modified expansion protocol for PB-CD19-CAR-T cells.[38] Thereafter, the phenotypes and the expression of exhaustion marker on the PB-GD2-CAR-T cells were assessed using flow cytometry. PB-GD2-CAR-T cells were successfully generated with a positivity rate of 44.1% ± 6.8% for PB-GD2-CAR at day 14 after transfection. Notably, PD-1 was scarcely expressed on PB-GD2-CAR-T cells (3.5% ± 1.1% in CAR-positive T cells), and

PB-GD2-CAR-T cells were predominantly (45.6% ± 5.6%) CD45RA/CCR7 positive (naïve/stem cell memory phenotype) (Figure 1B).

3.2 | Cytotoxicity of PB-GD2-CAR-T cells against GD2$^+$ NB cells

The ability of PB-GD2-CAR-T cells to kill tumor cells in coculture assays was evaluated. These cells were cocultured with the NB cell lines expressing GD2 at different levels, and the number of live tumor cells was measured by flow cytometry using counting beads. SH-SY5Y and IMR32 cells showed homogeneous expression of GD2; however, the expression in SK-N-AS cells was heterogeneous, with the cell population ranging from GD2$^-$ to GD2-high (Figure S1A). PB-GD2-CAR-T cells showed rapid and strong killing activity in these three NB cell lines (Figure 1C) but not in the GD2$^-$ SK-N-AS population (Figure S1B). This suggests that GD2-CAR-T cells have specific antitumor effects against GD2$^+$ tumors, and that the resistance of GD2-CAR-T cells is attributed to the heterogeneity of GD2 expression on tumor cells. Single-cell-derived AS-High cells were found to be more susceptible to GD2-CAR-T cells but were not eradicated with an increase in GD2-low clone, probably because of the immune escape due to the downregulation of GD2 (Figure S1C).

The sustained killing activity of PB-GD2-CAR-T cells was evaluated using the serial killing assay. PB-GD2-CAR-T cells showed strong and sustained killing activity against SH-SY5Y cells (Figure 1D), even after multiple tumor rechallenges without any mitigation of the antitumor efficacy by immune evasion, as is often observed for retrovirally engineered CAR-T cells.[39]

3.3 | Inhibition of the RAS/MEK pathway ameliorates the cytotoxic activity of PB-GD2-CAR-T cells in vitro

To investigate the effect of MEK inhibitors on NB cells, we incubated three NB cell lines having different mutation status of the MAPK pathway (Table S1) in the presence of trametinib, and monitored the growth of the cells with an xCELLigence real-time cell analyzer. The NRAS-mutated SK-N-AS cells were sensitive to trametinib at 10 nM, whereas the RAS-nonmutated IMR32 cells were resistant to it, and the other RAS-nonmutated SH-SY5Y line was partially sensitive at high concentrations of trametinib (Figure S2A). We also tested another RAS/MEK pathway inhibitor, CH5126766, which affects both the Raf and RAS/MEK pathways, against these NB cells. A similar sensitivity to the drug according to the mutation status of RAS/MEK pathway was observed (Figure S2B). Based on these data and previous reports,[9,36,40,41] we used these drugs at a concentration of 10 or 100 nM for our in vitro study.

To evaluate the effect of inhibition of the MEK pathway on PB-GD2-CAR-T cells, PB-GD2-CAR-T cells were cocultured with NB cell lines in the presence of trametinib, and the killing efficacy of PB-GD2-CAR-T cells against the NB cells was evaluated. When PB-GD2-CAR-T cells were cocultured with NB cells in the presence of 10 nM trametinib, the killing activity of PB-GD2-CAR-T cells was greatly inhibited (Figure 2A), although trametinib did not affect the expression of GD2 (Figure S3A) nor PD-L1 (Figure S3B) on the tumor cells. The suppression of the killing effect of PB-GD2-CAR-T cells was observed immediately after treatment with trametinib (Figure 2B). The other RAS/MEK inhibitor, CH5126766, also showed a rapid inhibition of the killing activity of PB-GD2-CAR-T cells (Figure S2C). The phosphorylation of ERK1/2, which operate downstream in the RAS-ERK signaling pathway and are associated with the activation of CAR-T cells, was induced in activated PB-GD2-CAR-T cells, whereas ERK1/2 phosphorylation was suppressed in the presence of trametinib (Figure 2C). Moreover, the production of inflammatory cytokines in PB-GD2-CAR-T cells was also inhibited following addition of trametinib (Figure 2D). Coculture of NB and PB-GD2-CAR-T cells greatly induced the expression of PD-1/Tim3/LAG3 in PB-GD2-CAR-T cells and of PD-L1 in NB cells, indicating the activation of immune evasion of NB cells. In contrast, addition of trametinib modestly suppressed the expression of the canonical T cell exhaustion markers including PD-1/Tim3/LAG3 in PB-GD2-CAR-T cells, and of PD-L1 in NB cells at low concentrations (Figures 2E and S3C). Because CAR-T cells could also induce HLA/TCR-dependent cytotoxicity and the downregulation of HLA class I molecules would be one of the immune evasion mechanisms, we evaluated the possible downregulation of HLA class I molecules by trametinib on NB tumor cells. The expression of HLA class I molecules on NB cells was not affected in the presence of trametinib, which could exclude the possibility of immune evasion through the downregulation of HLA class I molecules (Figure S4A,B). Notably, trametinib did not suppress the proliferation of PB-GD2-CAR-T cells after coculture with the tumor cells (Figure 2F). These data indicate that the inhibition of the RAS/MAPK pathway in PB-GD2-CAR-T cells reduced the cytotoxicity without the induction of canonical T cell exhaustion markers in vitro, but did not affect the proliferation of these T cells.

3.4 | In vivo effect of combination therapy with PB-GD2-CAR-T cells and trametinib

To verify the antitumor effect of PB-GD2-CAR-T cells and/or trametinib against GD2$^+$ tumors in a xenograft model, we engrafted AS-High-FFLuc cells into SCID Beige mice by subcutaneous injection. After the confirmation of tumor engraftment, mice were divided into four experimental groups (Figure 3A). PB-GD2-CAR-T cells were injected into the tail vein, and 1 mg/kg trametinib or vehicle was given orally to mice for 7 days. As anticipated, the growth of AS-High-FFLuc tumor treated with PB-GD2-CAR-T cells or trametinib was delayed, compared with that in control mouse (Figure 3B). However, unlike in the in vitro study, the combination of PB-GD2-CAR-T cells and trametinib efficiently controlled the growth of tumor and extended the survival of mice in this group (Figure 3B,C).

To determine the optimal timing of CAR-T cell injection in combination therapy, we additionally compared the proliferation of the

simultaneous treatment group injected with PB-GD2-CAR-T cells on day 0 at the same time starting trametinib for 7 days (the same experimental design as in the previous study shown in Figure 3), and pretreatment group with trametinib treatment for 7 days before CAR-T cell injection (Figure 4A). There was no significant difference in survival between the two groups, but the survival in the two groups

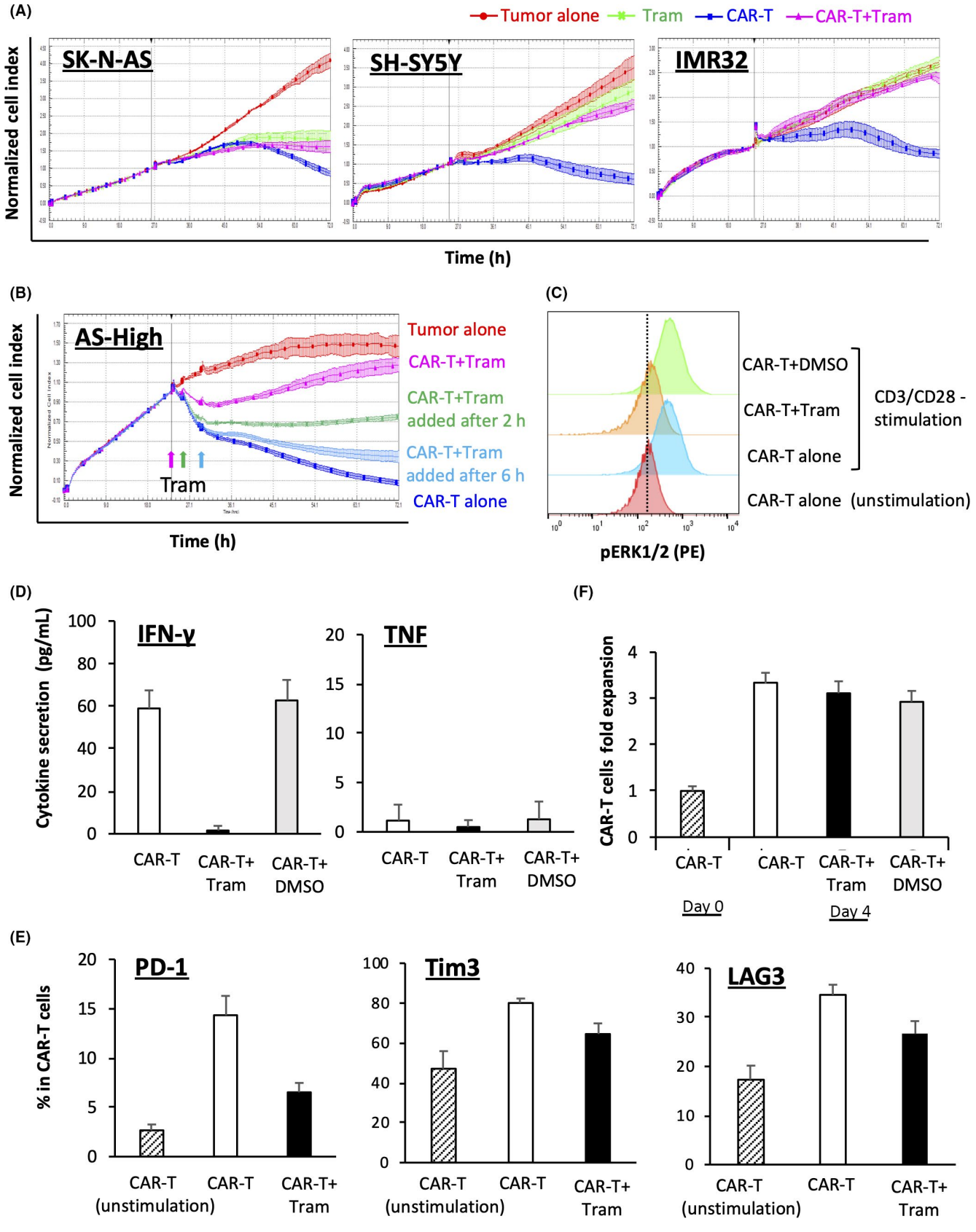

FIGURE 2 Trametinib inhibits the activity of *piggyBac*-mediated disialoganglioside GD2-specific chimeric antigen receptor-T (PB-GD2-CAR-T) cells in vitro. A, An impedance-based tumor cell killing assay. GD2-positive neuroblastoma cell lines were cocultured with PB-GD2-CAR-T cells and/or trametinib (Tram; 10 nM) at an effector : target (E:T) ratio of 2:1 in triplicate. Real-time impedance traces of tumor cells without treatment (Tumor alone; red), and tumor cells cocultured with Tram (light green), PB-GD2-CAR-T cells (CAR-T; blue), or PB-GD2-CAR-T cells and Tram (CAR-T+Tram; pink) were acquired for 72 h. B, Additional effects of trametinib on the killing activity of PB-GD2-CAR-T cells against GD2-high SK-N-AS cells (AS-High). Real-time impedance traces of tumor cells without treatment (red), and tumor cells cocultured with PB-GD2-CAR-T cells (blue), PB-GD2-CAR-T cells to which Tram was added at the same time (pink), after 2 h (green), or after 6 h (light blue) were acquired for 72 h. C, ERK 1/2 phosphorylation in $CD3^+$ T cells after coculture with Tram (100 nM). PB-GD2-CAR-T cells were cultured in the presence of Tram or DMSO (control) for 48 h with plate-bound CD3/CD28 Ab. D, Cytokine release assay. Production of inflammatory cytokines, γ-interferon (IFN-γ) and tumor necrosis factor (TNF), in PB-GD2-CAR-T cells after 48 h coculture with SH-SY5Y. E, Expression of programmed cell death-1 (PD-1), Tim3, and LAG3 in PB-GD2-CAR-T cells. PB-GD2-CAR-T cells were cultured for 48 h without SH-SY5Y (unstimulated), or with SH-SY5Y in the presence or absence of Tram. F, Additional effects of Tram on the proliferation of PB-GD2-CAR-T cells. PB-GD2-CAR-T cells on day 14 were cultured for 96 h in the presence of Tram or DMSO (control) in triplicate. The number of CAR-T cells on day 18 was measured by Cell Counter model R1 (Olympus)

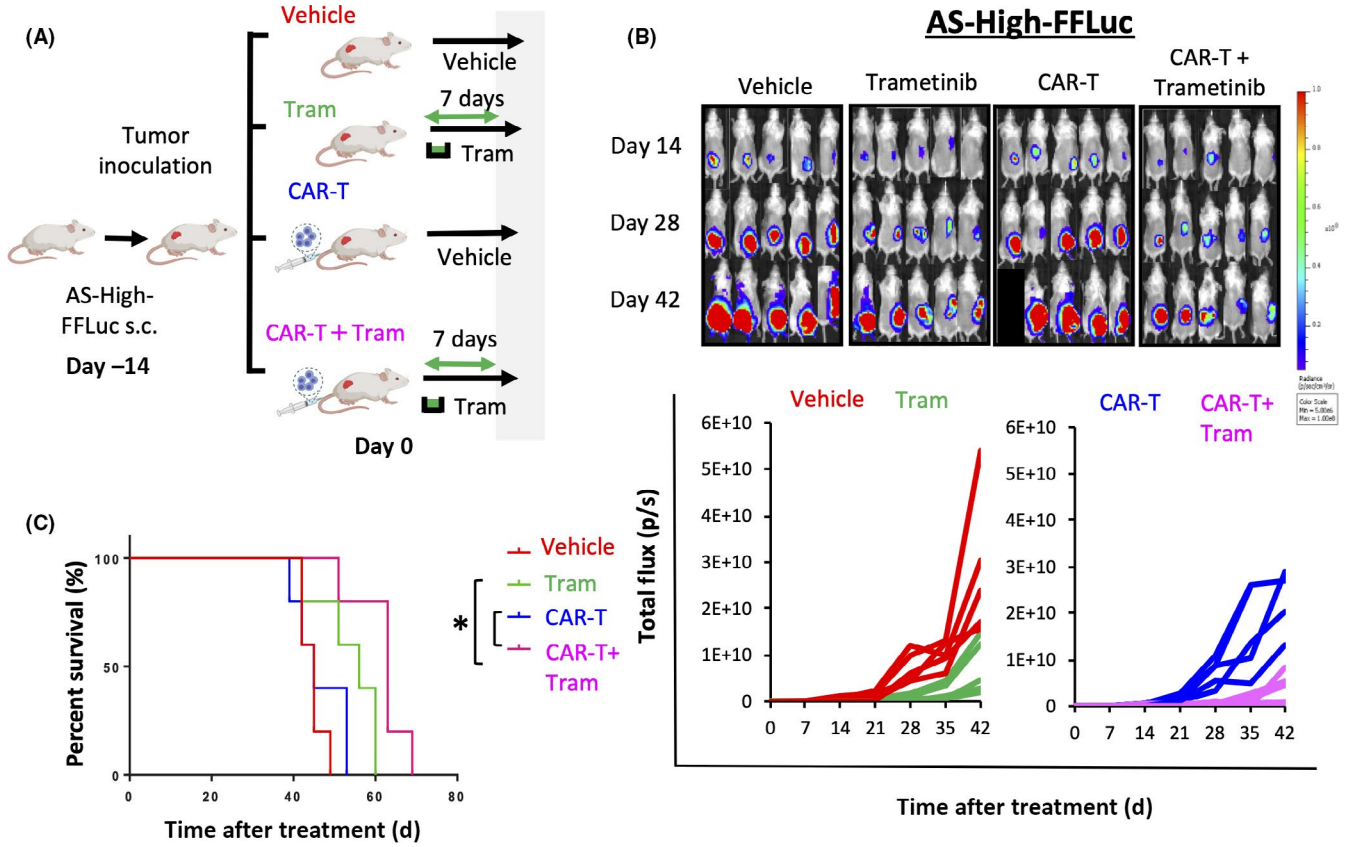

FIGURE 3 Combined therapy of *piggyBac*-mediated disialoganglioside GD2-specific chimeric antigen receptor-T (PB-GD2-CAR-T) cells with trametinib (Tram) delays tumor growth in vivo. A, Schematics of tumor challenge experiments in the xenograft model. After AS-High-FFluc tumor engraftment, mice were divided into four experimental groups (n = 5), as indicated. B, Tumor growth was measured as bioluminescence signal intensity and expressed as total flux (p/s). The combination treatment group showed a statistically significant reduction in tumor growth, measured as the mean total flux at day 43 (*) relative to the PB-GD2-CAR-T cell group. C, Survival curves for each treatment group (n = 5). The experiment was carried out twice, and representative results are shown here. $^*P < .05$

was extended more than that in the trametinib monotherapy group (Figure 4B). We also used the pretreatment strategy against large tumors (approximately 1×10^{10} p/s total flux), and compared the rate of total flux change every other week, with or without CAR-T cell injection (Figure 4C). In all the mice treated with trametinib alone, tumors regrew until day 21, whereas in mice injected with CAR-T cells following pretreatment, tumor regrowth was delayed (Figure 4D).

We also evaluated the antitumor effect of combined therapy in a RAS-nonmutated SH-SY5Y tumor xenograft model. SY5Y-FFLuc cells were engrafted into SCID Beige mice, and after the confirmation of tumor engraftment, these mice were divided into four experimental groups, same as in the previous experiment (Figures 5A and S5A). Interestingly, the effect of the combination therapy with PB-GD2-CAR-T cells and trametinib was also observed in SY5Y-FFLuc mice (Figures 5B,C and S5B). Taken together, addition of trametinib suppressed the killing activity of CAR-T cells in vitro, and showed synergistic effects with CAR-T cells in vivo, regardless of pre- or simultaneous treatment and the mutation status of the MAPK pathway in tumor cells.

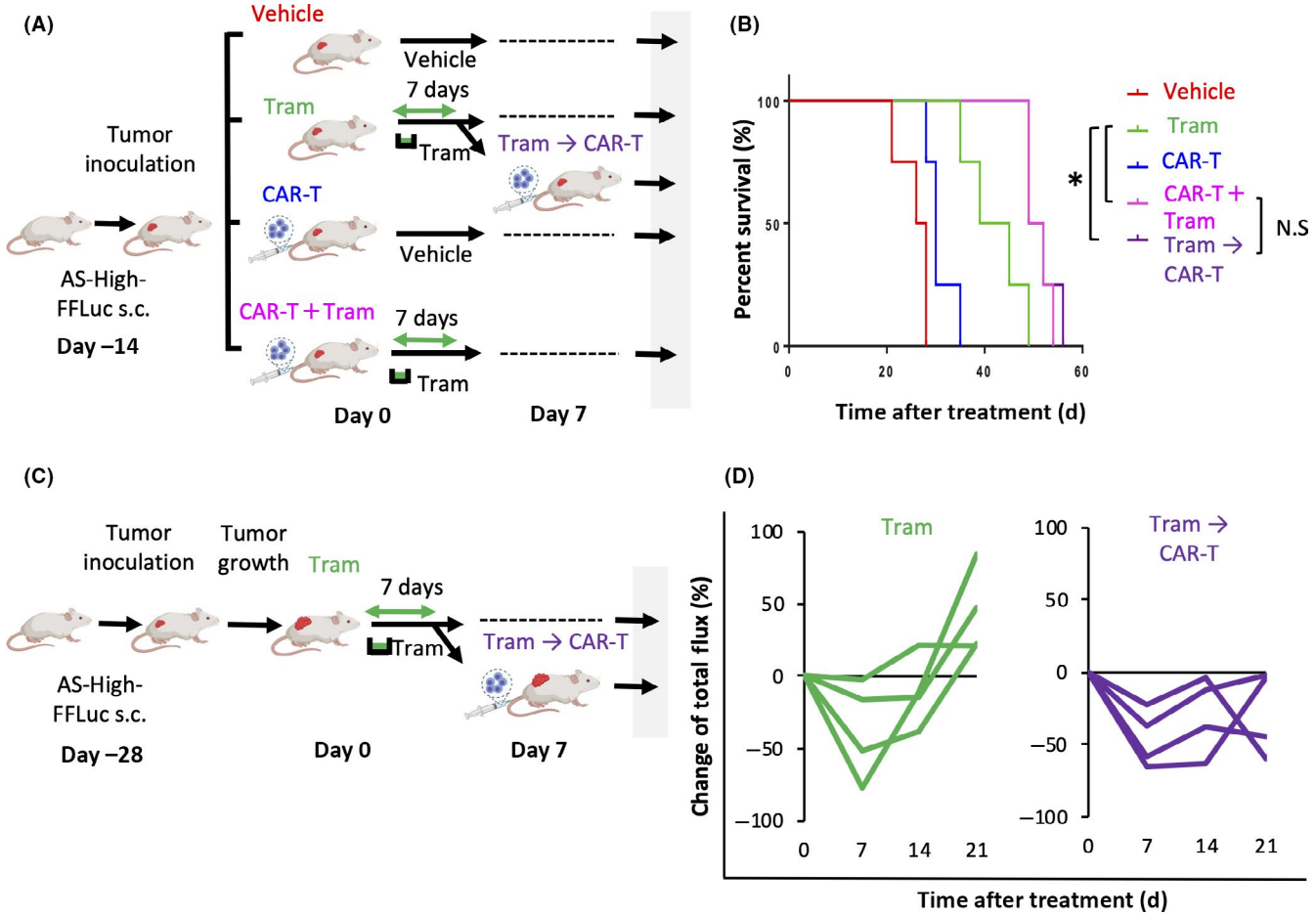

FIGURE 4 Pretreatment with trametinib (Tram) synergizes the antitumor effect of *piggyBac*-mediated disialoganglioside GD2-specific chimeric antigen receptor-T (PB-GD2-CAR-T) cells. A, Schematics of tumor challenge experiments in the xenograft model. After AS-High-FFluc tumor engraftment, mice were divided into five experimental groups (n = 4), as indicated. B, Survival curves for simultaneous treatment and pretreatment groups (n = 4). C, Schematics of tumor challenge experiments in the xenograft model. After AS-High-FFluc tumor engraftment and tumor growth, mice were divided into two experimental groups (n = 4), as indicated. D, Total flux change after the treatment with or without the injection of PB-GD2-CAR-T cells following Tram treatment for 7 days (n = 4). The experiment was undertaken twice, and representative results are shown here. *$P < .05$. NS, not significant ($P > .05$)

4 | DISCUSSION

In this study, we show that the MEK inhibitor, trametinib, ameliorates the killing efficacy of PB-GD2-CAR-T cells in vitro, whereas combined treatment with trametinib and PB-GD2-CAR-T cells showed superior antitumor efficacy in a murine xenograft model compared with PB-GD2-CAR-T cell monotherapy. Notably, this synergistic effect was also observed in the SH-SY5Y tumor xenograft model, which did not have MAPK pathway mutation and was resistant to trametinib, suggesting that the enhancement of the antitumor activity would not be developed by the direct killing activity of trametinib, but by the modulation of the immune evasion mechanism, which could impair the function of CAR-T cells. Therefore, this study should provide new insights about the feasibility of the combined treatment with CAR-T cells and MEK inhibitors, regardless of the mutation status of the MAPK pathway in tumor cells.

The MEK inhibitors have been successfully applied for various tumors with MAPK pathway mutations. The first generation MEK inhibitor, trametinib, remarkably improved the progression-free and overall survival rates among melanoma patients,[28] and various efforts have been made to apply MEK inhibitors to other cancers, including lung, ovarian, and pancreatic cancers, as a monotherapy or in combination with another molecular-targeting drugs.[42,43] The combined treatment of MEK inhibitor and ICI or T cell-mediated immunotherapy has also been investigated; however, the effect of MEK inhibitors on the functioning of T cells in in vitro studies remains controversial.[9,41,44] Previous reports revealed that MEK inhibitor is likely to inhibit the T-cell effector function in vitro,[9] which has limited the assessment combinations of MEK inhibitors and immunotherapies, even though the study lacked in vivo validation in a murine xenograft model. In our in vitro experiment, trametinib suppressed the phosphorylation of ERK1/2 on activated PB-GD2-CAR-T cells and production of IFN-γ and TNF, and completely impaired the antitumor activity of PB-GD2-CAR-T cells, consistent with the fact that MAPK signaling occurs downstream of T-cell receptor activation. Additionally, MEK inhibitors could impair the production of

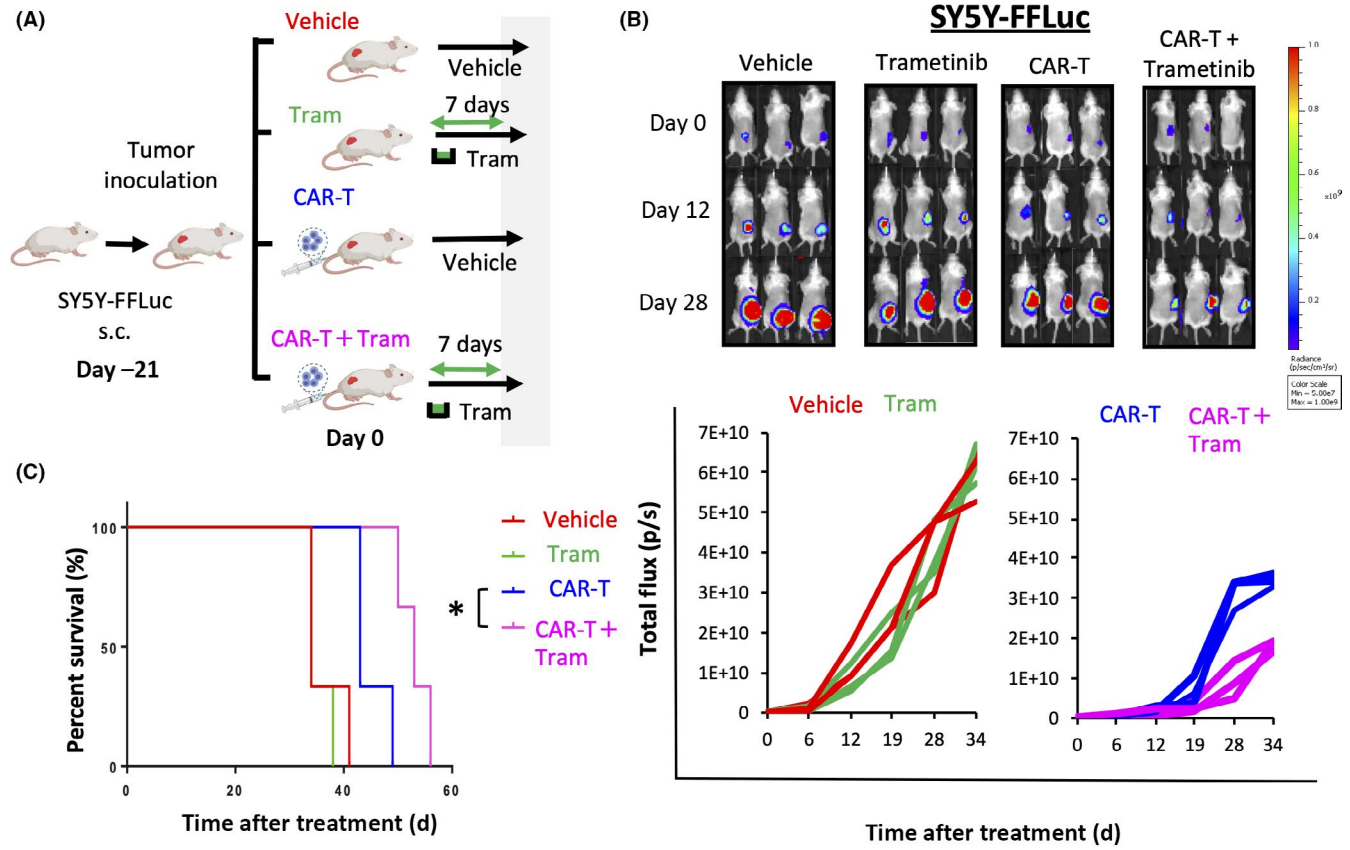

FIGURE 5 Combined therapy with *piggyBac*-mediated disialoganglioside GD2-specific chimeric antigen receptor-T (PB-GD2-CAR-T) cells and trametinib delays tumor growth even in MAPK pathway nonmutated tumor mouse. A, Schematics of tumor challenge experiments in the xenograft model. After SY5Y-FFluc tumor engraftment, mice were divided into four experimental groups (n = 3), as indicated. B, Tumor growth was measured as bioluminescence signal intensity and expressed as total flux (p/s). The combination treatment group showed a statistically significant reduction in tumor growth measured as the mean total flux at day 34 (*) relative to the PB-GD2-CAR-T cell group. C, Survival curves for each treatment group (n = 3). *$P < .05$

cytokines in T cells, whereas the MEK inhibitor did not affect the proliferation of PB-GD2-CAR-T cells. In contrast, recent studies have reported a synergistic effect of the MEK inhibitor, trametinib, on ICI[45] or B7-H3 redirected bispecific Ab, even in an in vitro study.[44] This controversy could be explained by the fact that trametinib selectively blocked the activation of naive T cells but did not suppress effector T cells, which were already activated.[45] Because the PB-GD2-CAR-T cells used by us showed a dominant fraction of naïve/stem cell memory T cells, the function of CAR-T cells was susceptible for impairment by trametinib, at least in our in vitro study. Nevertheless, recent studies have also determined the effectiveness of concurrent and sequential combinations of MEK inhibitors and ICI or T cell-mediated immunotherapy in murine xenograft models and also in clinical trials.[44-46] The precise mechanisms for the synergistic effect of MAPK pathway inhibition and ICI or T cell-mediated immunotherapy in vivo remain underexplored; however, recent studies have revealed that MEK inhibitor would augment the infiltration of CTLs at tumor sites, potentiate the antitumor function of T cells by impairing the activation-induced cell death, and upregulate the expression of MHC and PD-L1 on tumor cells,[31,47-49] which highlight the usefulness of MEK inhibitor in combination with ICI or T cell-mediated immunotherapy. However, our in vitro experiments revealed that the downregulation of PD-L1 on NB cells by trametinib was poorly involved with the mechanisms of enhanced antitumor effect of PB-GD2-CAR-T cells (Figure S6). Interestingly, recent studies have reported that MEK inhibitors transiently block MAPK signaling during the initial activation of T cells, and this delays the kinetics of T cell activation and cytokine secretion in vitro[9,40,47]; however, the long-term effects of MEK inhibitor on T cell function could not be explored in the in vitro experiment. Therefore, the in vitro data of short-term exposure of T cells to MEK inhibitor should be carefully evaluated and cannot be directly translated in vivo. Moreover, in a recent study, it was reported that transient inhibition of CAR signaling by blocking the downstream of TCRζ signaling can enhance the in vivo fitness of CAR-T cells by preventing exhaustion.[50] Indeed, in our murine xenograft model, either the simultaneous or preadministration of trametinib synergized the antitumor effect of PB-GD2-CAR-T cells regardless of the mutation status of the MAPK pathway. Although we have not explored the detailed kinetics of PB-GD2-CAR-T cells in vivo nor the biology of the tumor microenvironment, which are the main limitations of this study, our data should support previous observations that trametinib could not only directly inhibit tumors with mutated MAPK pathway but it also has some immunomodulatory function that could enhance the efficacy of ICI and

T cell-mediated immunotherapy. Taken together, our data support the potential for synergy between MAPK pathway inhibition and PB-GD2-CAR-T therapy for treatment of NB.

In conclusion, we present the potential synergistic benefits of PB-GD2-CAR-T cells and MEK inhibitors for clinical treatment of NB. Simultaneous or phased sequential treatment with trametinib enhanced the antitumor efficacy of PB-GD2-CAR-T cells regardless of the mutation status of the MAPK pathway. The combination of molecular-targeted therapy with immunotherapy could complement their modes of action, and achieve rapid but sustained tumor control with therapeutic synergy. Therefore, the combination of MEK inhibitors with CAR-T cell therapy is promising, and clinical studies are warranted to test the combination of these therapies in patients with refractory NB.

ACKNOWLEDGEMENTS

The authors acknowledge Dr Yohei Sugimoto and Ms Mami Kotoura for their valuable technical assistance and Ms Mika Tanimura and Ms Ryoko Murata for their secretarial assistance. The authors also thank Editage for proofreading, editing, and reviewing this manuscript. This work was supported by JSPS KAKENHI (20K07461). All illustrations were created with Biorender.com.

DISCLOSURE

The authors have no financial conflicts of interest related to this study.

DATA AVAILABILITY STATEMENT

The data that support the findings of this study are available from the corresponding author upon reasonable request.

ORCID

Akimasa Tomida https://orcid.org/0000-0001-6735-9681
Shigeki Yagyu https://orcid.org/0000-0003-4256-9783
Yozo Nakazawa https://orcid.org/0000-0003-0793-815X
Tomoko Iehara https://orcid.org/0000-0003-1740-7096

REFERENCES

1. Porter DL, Levine BL, Kalos M, Bagg A, June CH. Chimeric antigen receptor-modified T cells in chronic lymphoid leukemia. *New Engl J Med*. 2011;365:725-733.
2. Brentjens RJ, Rivière I, Park JH, et al. Safety and persistence of adoptively transferred autologous CD19-targeted T cells in patients with relapsed or chemotherapy refractory B-cell leukemias. *Blood*. 2011;118:4817-4828.
3. Kochenderfer JN, Dudley ME, Feldman SA, et al. B-cell depletion and remissions of malignancy along with cytokine-associated toxicity in a clinical trial of anti-CD19 chimeric-antigen-receptor-transduced T cells. *Blood*. 2012;119:2709-2720.
4. Lee DW, Kochenderfer JN, Stetler-Stevenson M, et al. T cells expressing CD19 chimeric antigen receptors for acute lymphoblastic leukaemia in children and young adults: a phase 1 dose-escalation trial. *Lancet*. 2015;385:517-528.
5. Brown CE, Badie B, Barish ME, et al. Bioactivity and safety of IL13Rα2-redirected chimeric antigen receptor CD8+ T cells in patients with recurrent glioblastoma. *Clin Cancer Res*. 2015;21:4062-4072.
6. Ahmed N, Brawley V, Hegde M, et al. HER2-specific chimeric antigen receptor-modified virus-specific T cells for progressive glioblastoma: a phase 1 dose-escalation trial. *JAMA Oncol*. 2017;3:1094-1101.
7. Schulz G, Cheresh DA, Varki NM, et al. Detection of ganglioside GD2 in tumor tissues and sera of neuroblastoma patients. *Cancer Res*. 1984;44:5914-5920.
8. Dobrenkov K, Ostrovnaya I, Gu J, Cheung IY, Cheung N-KV. Oncotargets GD2 and GD3 are highly expressed in sarcomas of children, adolescents, and young adults. *Pediatr Blood Cancer*. 2016;63:1780-1785.
9. Gargett T, Fraser CK, Dotti G, Yvon ES, Brown MP. BRAF and MEK inhibition variably affect GD2-specific chimeric antigen receptor (CAR) T-cell function in vitro. *J Immunother*. 2015;38:12-23.
10. Park JR, DiGiusto DL, Slovak M, et al. Adoptive transfer of chimeric antigen receptor re-directed cytolytic T lymphocyte clones in patients with neuroblastoma. *Mol Ther*. 2007;15:825-833.
11. Pule MA, Savoldo B, Myers GD, et al. Virus-specific T cells engineered to coexpress tumor-specific receptors: persistence and antitumor activity in individuals with neuroblastoma. *Nat Med*. 2008;14:1264-1270.
12. Louis CU, Savoldo B, Dotti G, et al. Antitumor activity and long-term fate of chimeric antigen receptor-positive T cells in patients with neuroblastoma. *Blood*. 2011;118:6050-6056.
13. Heczey A, Louis CU, Savoldo B, et al. CAR T cells administered in combination with lymphodepletion and PD-1 inhibition to patients with neuroblastoma. *Mol Ther*. 2017;25:2214-2224.
14. Long AH, Haso WM, Shern JF, et al. 4–1BB costimulation ameliorates T cell exhaustion induced by tonic signaling of chimeric antigen receptors. *Nat Med*. 2015;21:581-590.
15. Asgharzadeh S, Salo JA, Ji L, et al. Clinical significance of tumor-associated inflammatory cells in metastatic neuroblastoma. *J Clin Oncol*. 2012;30:3525-3532.
16. Long AH, Highfill SL, Cui Y, et al. Reduction of MDSCs with all-trans retinoic acid improves CAR therapy efficacy for sarcomas. *Cancer Immunol Res*. 2016;4:869-880.
17. Dong H, Strome SE, Salomao DR, et al. Tumor-associated B7–H1 promotes T-cell apoptosis: a potential mechanism of immune evasion. *Nat Med*. 2002;8:793-800.
18. Zou W, Chen L. Inhibitory B7-family molecules in the tumour microenvironment. *Nat Rev Immunol*. 2008;8:467-477.
19. Moon EK, Wang L-C, Dolfi DV, et al. Multifactorial T-cell hypofunction that is reversible can limit the efficacy of chimeric antigen receptor-transduced human T cells in solid tumors. *Clin Cancer Res*. 2014;20:4262-4273.
20. Majzner RG, Simon JS, Grosso JF, et al. Assessment of programmed death-ligand 1 expression and tumor-associated immune cells in pediatric cancer tissues. *Cancer*. 2017;123:3807-3815.
21. Bocca P, Di Carlo E, Caruana I, et al. Bevacizumab-mediated tumor vasculature remodelling improves tumor infiltration and antitumor efficacy of GD2-CAR T cells in a human neuroblastoma preclinical model. *OncoImmunology*. 2018;7:1-11.
22. Spurny C, Kailayangiri S, Jamitzky S, et al. Programmed cell death ligand 1 (PD-L1) expression is not a predominant feature in Ewing sarcomas. *Pediatr Blood Cancer*. 2018;65:e26719.
23. Eleveld TF, Oldridge DA, Bernard V, et al. Relapsed neuroblastomas show frequent RAS-MAPK pathway mutations. *Nat Genet*. 2015;47:864-871.
24. Tanaka T, Higashi M, Kimura K, et al. MEK inhibitors as a novel therapy for neuroblastoma: their in vitro effects and predicting their efficacy. *J Pediatr Surg*. 2016;51:2074-2079.
25. Takeuchi Y, Tanaka T, Higashi M, et al. In vivo effects of short- and long-term MAPK pathway inhibition against neuroblastoma. *J Pediatr Surg*. 2018;53:2454-2459.
26. Zeiser R, Andrlová H, Meiss F. Trametinib (GSK1120212). Recent Results Cancer Res. 211:91-100.

27. Kieran MW, Geoerger B, Dunkel IJ, et al. A phase I and pharmacokinetic study of oral dabrafenib in children and adolescent patients with recurrent or refractory BRAF V600 mutation–positive solid tumors. *Clin Cancer Res*. 2019;25:7294-7302.
28. Flaherty KT, Robert C, Hersey P, et al. Improved survival with MEK inhibition in BRAF-mutated melanoma. *New Engl J Med*. 2012;367:107-114.
29. Hodi FS, O'Day SJ, McDermott DF, et al. Improved survival with ipilimumab in patients with metastatic melanoma. *New Engl J Med*. 2010;363:711-723.
30. Hu-Lieskovan S, Mok S, Homet Moreno B, et al. Improved antitumor activity of immunotherapy with BRAF and MEK inhibitors in BRAF(V600E) melanoma. *Sci Transl Med*. 2015;7:279ra41.
31. Loi S, Dushyanthen S, Beavis PA, et al. RAS/MAPK activation is associated with reduced tumor-infiltrating lymphocytes in triple-negative breast cancer: therapeutic cooperation between MEK and PD-1/PD-L1 immune checkpoint inhibitors. *Clin Cancer Res*. 2016;22:1499-1509.
32. Ribas A, Lawrence D, Atkinson V, et al. Combined BRAF and MEK inhibition with PD-1 blockade immunotherapy in BRAF-mutant melanoma. *Nat Med*. 2019;25:936-940.
33. Jiang X, Zhou J, Giobbie-Hurder A, Wargo J, Hodi FS. The activation of MAPK in melanoma cells resistant to BRAF inhibition promotes PD-L1 expression that is reversible by MEK and PI3K inhibition. *Clin Cancer Res*. 2013;19:598-609.
34. Yamamoto R, Nishikori M, Tashima M, et al. B7–H1 expression is regulated by MEK/ERK signaling pathway in anaplastic large cell lymphoma and Hodgkin lymphoma. *Cancer Sci*. 2009;100:2093-2100.
35. Berthon C, Driss V, Liu J, et al. In acute myeloid leukemia, B7–H1 (PD-L1) protection of blasts from cytotoxic T cells is induced by TLR ligands and interferon-gamma and can be reversed using MEK inhibitors. *Cancer Immunol Immunother*. 2010;59:1839-1849.
36. Umapathy G, Guan J, Gustafsson DE, et al. MEK inhibitor trametinib does not prevent the growth of anaplastic lymphoma kinase (ALK)-addicted neuroblastomas. *Sci Signal*. 2017;10:eaam7550.
37. Nakazawa Y, Huye LE, Dotti G, et al. Optimization of the PiggyBac transposon system for the sustained genetic modification of human T lymphocytes. *J Immunother*. 2009;32:826-836.
38. Morita D, Nishio N, Saito S, et al. Enhanced expression of anti-CD19 chimeric antigen receptor in piggyBac transposon-engineered T cells. *Mol Ther*. 2018;8:131-140.
39. Tanaka M, Tashiro H, Omer B, et al. Vaccination targeting native receptors to enhance the function and proliferation of Chimeric Antigen Receptor (CAR)-modified T cells. *Clinl Cancer Res*. 2017;23:3499-3509.
40. Dushyanthen S, Teo ZL, Caramia F, et al. Agonist immunotherapy restores T cell function following MEK inhibition improving efficacy in breast cancer. *Nat Commun*. 2017;8:606.
41. Dörrie J, Babalija L, Hoyer S, et al. BRAF and MEK inhibitors influence the function of reprogrammed T cells: consequences for adoptive T-cell therapy. *Int J Mol Sci*. 2018;19:289.
42. Jing J, Greshock J, Holbrook JD, et al. Comprehensive predictive biomarker analysis for MEK inhibitor GSK1120212. *Mol Cancer Ther*. 2012;11:720-729.
43. Drosten M, Barbacid M. Targeting the MAPK pathway in KRAS-driven tumors. *Cancer Cell*. 2020;37:543-550.
44. Li H, Huang C, Zhang Z, et al. MEK inhibitor augments antitumor activity of B7-H3-redirected bispecific antibody. *Front Oncol*. 2020;10:1527.
45. Liu LI, Mayes PA, Eastman S, et al. The BRAF and MEK Inhibitors Dabrafenib and Trametinib: effects on immune function and in combination with immunomodulatory antibodies targeting PD-1, PD-L1, and CTLA-4. *Clin Cancer Res*. 2015;21:1639-1651.
46. Choi H, Deng J, Li S, et al. Pulsatile MEK inhibition improves antitumor immunity and T cell function in murine Kras mutant lung cancer. *Cell Rep*. 2019;27:806-819.e5.
47. Ebert PJR, Cheung J, Yang Y, et al. MAP kinase inhibition promotes T cell and anti-tumor activity in combination with PD-L1 checkpoint blockade. *Immunity*. 2016;44:609-621.
48. Bommareddy PK, Aspromonte S, Zloza A, Rabkin SD, Kaufman HL. MEK inhibition enhances oncolytic virus immunotherapy through increased tumor cell killing and T cell activation. *Sci Transl Med*. 2018;10:eaau0417.
49. Moshofsky KB, Cho HJ, Wu G, et al. Acute myeloid leukemia-induced T-cell suppression can be reversed by inhibition of the MAPK pathway. *Blood adv*. 2019;3:3038-3051.
50. Weber EW, Parker KR, Sotillo E, et al. Transient rest restores functionality in exhausted CAR-T cells through epigenetic remodeling. *Science*. 2021;372:eaba1786.

SUPPORTING INFORMATION

Additional supporting information may be found online in the Supporting Information section.

How to cite this article: Tomida A, Yagyu S, Nakamura K, et al. Inhibition of MEK pathway enhances the antitumor efficacy of chimeric antigen receptor T cells against neuroblastoma. *Cancer Sci*. 2021;112:4026–4036. https://doi.org/10.1111/cas.15074